Journal of Rock Mechanics and Geotechnical Engineering 14 (2022) 144–152

Contents lists available at ScienceDirect

Journal of Rock Mechanics and Geotechnical Engineering

journal homepage: www.jrmge.cn

Full Length Article

Analytical computation of support characteristic curve for circumferential yielding lining in tunnel design

Kui Wu [a,b], Zhushan Shao [a,b,*], Mostafa Sharifzadeh [c,**], Siyuan Hong [b], Su Qin [b]

[a] School of Science, Xi'an University of Architecture and Technology, Xi'an, 710055, China
[b] Shaanxi Key Laboratory of Geotechnical and Underground Space Engineering (XAUAT), Xi'an University of Architecture and Technology, Xi'an, 710055, China
[c] Department of Mining and Metallurgical Engineering, Western Australian School of Mines, Curtin University, Kalgoorlie, 6430, Australia

ARTICLE INFO

Article history:
Received 5 January 2021
Received in revised form
4 April 2021
Accepted 10 June 2021
Available online 2 November 2021

Keywords:
Squeezing ground
Circumferential yielding lining
Highly deformable element
Support characteristic curve (SCC)
Analytical method

ABSTRACT

Circumferential yielding lining is able to tolerate controlled displacements without failure, which has been proven to be an effective solution to large deformation problem in squeezing tunnels. However, up to now, there has not been a well-established design method for it. This paper aims to present a detailed analytical computation of support characteristic curve (SCC) for circumferential yielding lining, which is a significant aspect of the implementation of convergence-confinement method (CCM) in tunnel support design. Circumferential yielding lining consists of segmental shotcrete linings and highly deformable elements, and its superior performance mainly depends on the mechanical characteristic of highly deformable element. The deformation behavior of highly deformable element is firstly investigated. Its whole deforming process can be divided into three stages including elastic, yielding and compaction stages. Especially in the compaction stage of highly deformable element, a nonlinear stress–strain relationship can be observed. For mathematical convenience, the stress–strain curve in this period is processed as several linear sub-curves. Then, the reasons for closure of circumferential yielding lining in different stages are explained, and the corresponding accurate equations required for constructing the SCC are provided. Furthermore, this paper carries out two case studies illustrating the application of all equations needed to construct the SCC for circumferential yielding lining, where the reliability and feasibility of theoretical derivation are also well verified. Finally, this paper discusses the sensitivity of sub-division in element compaction stage and the influence of element length on SCC. The outcome of this paper could be used in the design of proper circumferential yielding lining.

1. Introduction

Deep excavation in squeezing ground normally contributes to very high rock displacements, and if a stiff support concept is applied, very high bearing capacity is required. This has been proved to be both an uneconomic and an unsafe practice, resulting in extremely high lining thickness and lining brittle-violent failure (Radončić et al., 2009; Barla, 2016; Langford et al., 2016; Wu and Shao, 2019; Aygar, 2020; Wu et al., 2020a). The only feasible solution in heavily squeezing ground is a tunnel support that is able to tolerate controlled rock displacements without failure (Cantieni and Anagnostou, 2009; Wu et al., 2019, 2020b). In order to achieve such purpose, a novel support form, i.e. shotcrete lining embedded by highly deformable elements, was proposed and first applied in Galgenberg tunnel, Austria in 1994 (Schubert et al., 2018). In this support system, those elements show stronger deformability compared with shotcrete, and a reduction in the lining circumference is allowed upon loading due to considerable shortening of highly deformable elements, thus avoiding shotcrete failure – this is the so-called "circumferential yielding lining".

Due to significant advantages of circumferential yielding lining in the field of squeezing tunnel support, up to now, several different types of highly deformable elements have been sequentially developed and improved, for instance lining stress controller (LSC) (Moritz, 2011), telescope yielding element (Verient et al., 2015) and HidCon element (Barla et al., 2011). Based on the type of production

* Corresponding author. School of Science, Xi'an University of Architecture and Technology, Xi'an, 710055, China.
** Corresponding author.
E-mail addresses: shaozhushan@xauat.edu.cn (Z. Shao), m.sharifzadeh@curtin.edu.au (M. Sharifzadeh).
Peer review under responsibility of Institute of Rock and Soil Mechanics, Chinese Academy of Sciences.

https://doi.org/10.1016/j.jrmge.2021.06.016

material, these highly deformable elements can be categorized into two basic groups: porous elements based on binders and steel elements (Moritz, 2011). The concept of circumferential yielding lining has been successfully applied in many squeezing tunnels throughout the world (Thut et al., 2006; Kovári, 2009; Deng et al., 2020; Lu et al., 2021), and some application examples are shown in Fig. 1. The use of highly deformable element in shotcrete lining seems a simple task. In practice, it is rather challenging due to the time-dependent properties of shotcrete and time- and face-dependent development of tunnel closure (Paraskevopoulou and Diederichs, 2018; Fan et al., 2020; He et al., 2021; Sun et al., 2021). Even, it is an approach that can fail dramatically if used incorrectly (Asef et al., 2000). In Saint Martin La Porte access adit of Base tunnel connecting Lyon and Torino, the number and position of highly deformable elements in shotcrete lining were changed several times to fulfill the requirements of tunnel design and lining bearing capacity (Bonini and Barla, 2012). Many researchers attempted to predict the response of tunnels using the system of circumferential yielding lining. Ramoni and Anagnostou (2011) reported the tunnel response in different systems of circumferential yielding lining based on the numerical method. Tian et al. (2016, 2018) carried out a series of numerical investigations and discussed the influence of design parameters of highly deformable element on tunnel performance. Hasanpour et al. (2018) studied the interaction between circumferential yielding lining and squeezing ground by means of two different numerical approaches. Although it has been recognized as an effective measure for tunneling in squeezing ground, there is still no well-established design method for circumferential yielding lining (Hammer et al., 2018).

The convergence-confinement method (CCM) of support design is a convenient analytical-graphical procedure for estimating the required bearing capacity of tunnel support (Carranza-Torres and Engen, 2017; De La Fuente et al., 2019; Wang et al., 2021), particularly in the early stage of support design. This method consists in constructing ground reaction curve (GRC) based on the planned tunnel diameter, ground stress and rock mass quality, together with support characteristic curve (SCC) based on the support mechanical properties. Numerous studies on constructing GRC have been carried out by Brown et al. (1983), Wang (1996), Carranza-Torres (2003), Oreste (2003a), Kabwe et al. (2020a), and Xu and Xia (2021), among others. In their solutions, many different conditions were considered. Now, it is sufficient to make an easy and quick determination of the GRC based on the existing methods. In addition, because conventional stiff lining experienced a lengthy developing process, there have been many approaches to conveniently construct its SCC (Kumasaka, 2007; Oreste, 2003b; Oke et al., 2018; Yan et al., 2018; Lu and Sun, 2020; Kabwe et al., 2020b). Regarding some special support structures, Rodríguez and Díaz-Aguado (2013) attempted to propose accurate equations of the characteristic curve for yielding steel ribs. Carranza-Torres and Engen (2017) provided the analytical expression of the SCC for blocked steel sets. Due to the short time of development, few researches focused on the construction of SCC for circumferential lining, which seriously limits its wide application in squeezing tunnel engineering.

This paper pays attention to the analytical computation of SCC for circumferential lining. The mechanical behavior of highly deformable elements is fully analyzed. The reasons for closure of circumferential yielding lining in different stages are explained, and the corresponding accurate equations required for constructing the SCC are then provided. Furthermore, two case studies are carried out, illustrating the application of all proposed equations. Finally, a parametric investigation on highly deformable element is performed.

2. Ground reaction curve

As previously mentioned, the implementation of the CCM consists in constructing the GRC and SCC. The GRC actually exhibits the

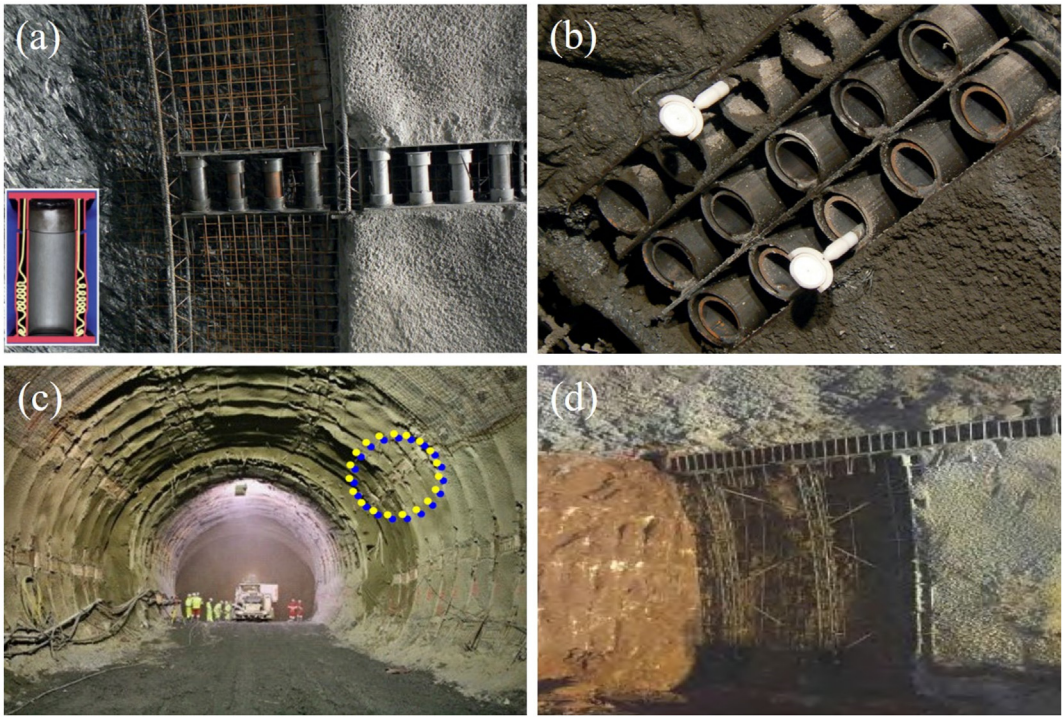

Fig. 1. Applications of circumferential yielding lining in tunnels: (a) Lining stress controller (LSC) (Moritz, 2011); (b) Wabe element (Radončić et al., 2009); (c) HidCon element (Barla et al., 2012); and (d) Support resistant limiting damper (SRLD) (Qiu et al., 2018).

relationship between support pressure and tunnel radial displacement. In a linear elastic ground, the expression of GRC is usually given by

$$u_r(x) = \lambda(x)u(\infty)_{\mathrm{ul}} \tag{1}$$

where $\lambda(x)$ is the displacement release coefficient closely associated with the rock property and tunnel face advancement, and its expression has been provided by many researchers (Chu et al., 2019, 2021); $u(\infty)_{\mathrm{ul}}$ represents the tunnel radial displacement far from the tunnel face in elastic geomaterial, which can be calculated as

$$u(\infty)_{\mathrm{ul}} = \frac{p_0 r_0}{2G} \tag{2}$$

where p_0 denotes the initial ground stress, r_0 is the tunnel radius, and G is the rock shear modulus.

When the Mohr–Coulomb yield criterion is satisfied, the computing formula of GRC for an elastoplastic ground is given as follows (Panet, 1995):

$$u_r(x) = \frac{(1+\nu)r_0}{E}\left[C_1 + C_2\left(\frac{r_0}{R_{\mathrm{pl}}}\right)^{K_{\mathrm{p}}-1} + C_3\left(\frac{r_0}{R_{\mathrm{pl}}}\right)^{\beta+1}\right] \tag{3}$$

$$C_1 = -(1-2\nu)(p_0+H) \tag{4}$$

$$C_2 = \left[\frac{(1-\nu)(1+\beta K_{\mathrm{p}})}{K_{\mathrm{p}}+\beta} - \nu\right]\frac{2(p_0+H)}{K_{\mathrm{p}}+1} \tag{5}$$

$$C_3 = 2(1-\nu)\frac{(K_{\mathrm{p}}-1)(p_0+H)}{K_{\mathrm{p}}+\beta} \tag{6}$$

$$R_{\mathrm{pl}} = \left[\frac{2(p_0+H)}{K_{\mathrm{p}}+1}\frac{r_0^{K_{\mathrm{p}}-1}}{(1-\lambda)p_0+H}\right]^{\frac{1}{K_{\mathrm{p}}-1}} \tag{7}$$

$$H = \frac{c}{\tan\varphi} \tag{8}$$

$$\beta = \frac{1+\sin\psi}{1-\sin\psi} \tag{9}$$

$$K_{\mathrm{p}} = \frac{1+\sin\varphi}{1-\sin\varphi} \tag{10}$$

where E and ν are the elastic modulus and Poisson's ratio of geomaterial, respectively; and c, φ and ψ denote the cohesion, friction angle and dilatancy angle, respectively.

3. Support characteristic curve for circumferential yielding lining

3.1. Highly deformable element behavior

Due to its low elastic modulus and strong deformability compared with shotcrete, major rock displacement can be absorbed by the highly deformable elements integrated into shotcrete lining. Fig. 2 shows the general stress–strain curves of highly deformable element, and its whole deforming process can be basically divided into three stages: elastic stage (I), yielding stage (II) and compaction stage (III). In the elastic stage (I), the strain of highly deformable element generally linearly increases with stress. This stage only lasts for a short time owing to its low yield stress.

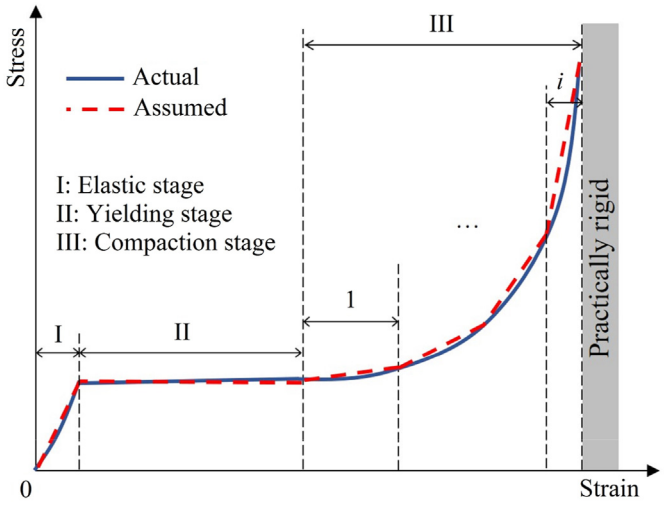

Fig. 2. Actual and assumed stress–strain curves for highly deformable elements.

Once the yield stress of highly deformable element is achieved, plastic strain occurs without stress increase. This is the yielding stage (II). As the strain continuously accumulates, highly deformable element subsequently enters its compaction stage, and in general a nonlinear stress–strain relationship can be observed in this stage, which indicates that the elastic modulus of highly deformable element is not a constant. When it experiences the maximum (limit) strain, highly deformable element eventually can be regarded as a practically rigid one.

As highly deformable element shows a nonlinear stress–strain relationship in compaction stage (III), its elastic modulus is not a constant, leading to the mathematical difficulty of analytical computation. According to Sakai and Schubert (2019), it is practical and feasible to divide the nonlinear curve in this period into i linear sub-curves, and then the simplified sub-curves are plotted in red dashed lines, as shown in Fig. 2. Accordingly, the elastic modulus of highly deformable element in this stage can be easily calculated.

3.2. Equation derivation for constructing support characteristic curve

Based on the theory of elasticity, the mean circumferential stress in a tunnel lining can be expressed in the form of external load as follows:

$$\sigma_\theta = \frac{p_i r_0}{t_{\mathrm{s}}} \tag{11}$$

where σ_θ denotes the mean circumferential stress in the lining, p_i is the rock pressure (support pressure), and t_{s} is the lining thickness.

For a circumferential lining subjected to rock pressure, its closure can be induced by two parts: shortenings of highly deformable elements and segmental shotcrete linings. The mechanical model of a circumferential yielding lining is illustrated in Fig. 3, where m is the number of highly deformable element. The radial displacement of this circumferential yielding lining can be given by

$$u_r = \varepsilon_{\theta,\mathrm{t}} r_0 \tag{12}$$

where u_r denotes the radial displacement; and $\varepsilon_{\theta,\mathrm{t}}$ represents the total circumferential strain of lining (including strains of highly deformable element and segmental shotcrete lining), which can be calculated as

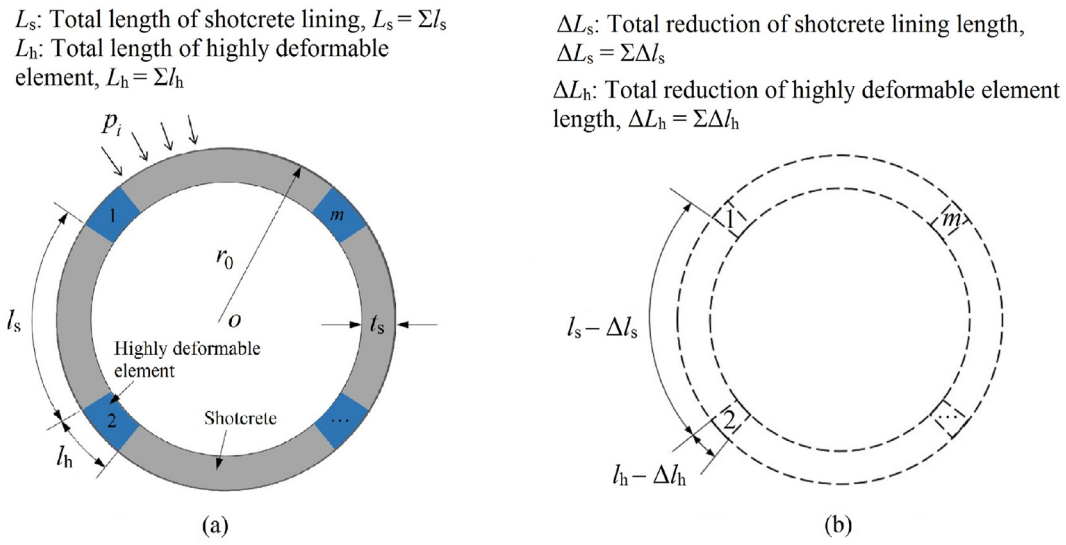

Fig. 3. Mechanical model of a circumferential yielding lining: (a) before and (b) after deformation.

$$\varepsilon_{\theta,t} = \frac{\Delta L}{L} = \frac{\Delta L_s + \Delta L_h}{2\pi r_0} \tag{13}$$

where L and ΔL are the lining length and its reduction, respectively; and ΔL_s and ΔL_h represent the reductions in the length of segmental shotcrete lining and highly deformable element, respectively.

The reduction in the length of segmental shotcrete lining ΔL_s can be expressed by

$$\Delta L_s = \varepsilon_{\theta,s}(2\pi r_0 - m l_h) = \frac{\sigma}{E_s}(2\pi r_0 - m l_h) \tag{14}$$

where $\varepsilon_{\theta,s}$ is the strain of shotcrete lining, l_h represents the length of each highly deformable element, and E_s is the elastic modulus of shotcrete. In practice, the reduced elastic modulus is usually used for analysis due to the time-dependency of shotcrete.

The reduction in the length of highly deformable element ΔL_h can be calculated as

$$\Delta L_h = \varepsilon_{\theta,h} m l_h \tag{15}$$

where $\varepsilon_{\theta,h}$ stands for the strain of highly deformable element.

On account of special deformation behavior of highly deformable element, its strain depends on the circumferential stress in the lining, which is expressed as

$$\varepsilon_{\theta,h} = f(\sigma_\theta) \tag{16}$$

When $\sigma_\theta < \sigma_y$ (the yield stress of highly deformable element), elastic deformation occurs, and the stress–strain relationship of highly deformable element satisfies the following equation:

$$\varepsilon_{\theta,h} = \frac{\sigma_\theta}{E_{h1}} \tag{17}$$

where E_{h1} denotes the elastic modulus of highly deformable element in the elastic stage.

Substituting Eq. (17) into Eq. (15) provides the shortening of highly deformable elements in the elastic stage as follows:

$$\Delta L_h = \frac{\sigma_\theta m l_h}{E_{h1}} \tag{18}$$

Combining Eqs. (11), (13), (14) and (18), the total lining circumferential strain in this stage can be given by

$$\varepsilon_{\theta,t} = \frac{p_i r_0}{E_s t_s}\left(1 - \frac{m l_h}{2\pi r_0}\right) + \frac{p_i m l_h}{2\pi E_{h1} t_s} \tag{19}$$

Furthermore, the expression of SCC for circumferential lining in the elastic stage, using Eqs. (12) and (19), can be obtained as

$$\frac{u_r}{p_i} = \frac{r_0^2}{E_s t_s}\left(1 - \frac{m l_h}{2\pi r_0}\right) + \frac{r_0 m l_h}{2\pi E_{h1} t_s} \tag{20}$$

If the circumferential stress in the lining σ_θ reaches the yield stress σ_y, this indicates that the yielding stage starts for highly deformable elements. In this stage, the closure of lining is totally induced by plastic shortening of highly deformable elements, and the lining circumferential stress therefore remains unchanged. The reduction in the length of shotcrete lining in the yielding stage keeps the value corresponding to that at $\sigma_\theta = \sigma_y$, as shown in Eq. (21). The shortening of highly deformable elements varies in a certain range, as shown in Eq. (22).

$$\Delta L_s = \frac{\sigma_y}{E_s}(2\pi r_0 - m l_h) \tag{21}$$

$$\frac{\sigma_y m l_h}{E_{h1}} < \Delta L_h < \varepsilon_{hy} m l_h \tag{22}$$

where ε_{hy} represents the strain of element when the yielding stage completes.

Subsequently, the total circumferential strain of lining in this stage varies within a range as follows:

$$\frac{\sigma_y}{E_s}\left(1 - \frac{m l_h}{2\pi r_0}\right) + \frac{\sigma_y m l_h}{2\pi r_0 E_{h1}} < \varepsilon_{\theta,t} < \frac{\sigma_y}{E_s}\left(1 - \frac{m l_h}{2\pi r_0}\right) + \frac{\varepsilon_{hy} m l_h}{2\pi r_0} \tag{23}$$

By using Eqs. (11), (12) and (23), the expression of SCC for circumferential yielding lining in the yielding stage can be written as

$$\left.\begin{aligned}&\frac{\sigma_y r_0}{E_s}\left(1-\frac{ml_h}{2\pi r_0}\right)+\frac{\sigma_y ml_h}{2\pi E_h}<u_r<\frac{\sigma_y r_0}{E_s}\left(1-\frac{ml_h}{2\pi r_0}\right)+\frac{\varepsilon_y ml_h}{2\pi}\\&p_i=\frac{\sigma_y t_s}{r_0}\end{aligned}\right\} \tag{24}$$

As previously mentioned, for mathematical convenience, the nonlinear stress–strain curve of highly deformable elements in the compaction stage can be processed as i linear sub-curves, and the elastic modulus corresponding to each linear stress–strain sub-curve can be considered to be equal to $E_{h3,i}$. Then, the shortening of highly deformable elements in the compaction stage can be calculated as follows:

$$\Delta L_h=\varepsilon_y ml_h+ml_h\left(\frac{\sigma_{\theta 3,1}-\sigma_y}{E_{h3,1}}+\ldots+\frac{\sigma_{\theta 3,i}-\sigma_{\theta 3,i-1}}{E_{h3,i}}\right) \tag{25}$$

where $\sigma_{\theta 3,i}$ denotes the circumferential stress in the lining in the ith step of compaction stage. The range of element length reduction in this stage is

$$\varepsilon_{hy}ml_h<\Delta L_h<\varepsilon_{hlim}ml_h \tag{26}$$

where ε_{hlim} stands for the limit strain of highly deformable element.

The corresponding reduction in the length of shotcrete lining in the compaction stage is

$$\Delta L_s=\varepsilon_{\theta,s}(2\pi r_0-ml_h)=\frac{\sigma_{\theta 3,i}}{E_s}(2\pi r_0-ml_h) \tag{27}$$

The total circumferential strain of lining in the compaction stage can be subsequently given by

$$\begin{aligned}\varepsilon_{\theta,t}=&\frac{\sigma_{\theta 3,i}}{2\pi r_0 E_s}(2\pi r_0-ml_h)+\frac{\varepsilon_y ml_h}{2\pi r_0}\\&+\frac{ml_h}{2\pi r_0}\left(\frac{\sigma_{\theta 3,1}-\sigma_y}{E_{h3,1}}+\ldots+\frac{\sigma_{\theta 3,i}-\sigma_{\theta 3,i-1}}{E_{h3,i}}\right)\end{aligned} \tag{28}$$

Substituting Eqs. (11) and (28) into Eq. (12) provides the expression of SCC for circumferential yielding lining in the compaction stage as follows:

$$\begin{aligned}u_r=&\frac{p_i r_0}{2\pi E_s t_s}(2\pi r_0-ml_h)+\frac{\varepsilon_{hy}ml_h}{2\pi}\\&+\frac{ml_h}{2\pi}\left(\frac{p_i r_0-\sigma_y t_s}{E_{h3,1}t_s}+\ldots+\frac{p_i r_0-\sigma_{\theta 3,i-1}t_s}{E_{h3,i}t_s}\right)\end{aligned} \tag{29}$$

When the highly deformable elements integrated into shotcrete lining experience their limit strain, they will become practically rigid and the gaps filled with these elements can be considered to be closed. Thereafter, the shortening of highly deformable elements keeps constant:

$$\Delta L_h=\varepsilon_{lim}ml_h \tag{30}$$

The reduction in the length of shotcrete lining after gaps closing still can be calculated using Eq. (14). The total circumferential strain of lining is formulated in Eq. (31) and then the expression of SCC is shown in Eq. (32).

$$\varepsilon_{\theta,t}=\frac{\sigma_\theta}{E_s}\left(1-\frac{ml_h}{2\pi r_0}\right)+\frac{\varepsilon_{hlim}ml_h}{2\pi r_0} \tag{31}$$

$$u_r=\frac{p_i r_0^2}{E_s t_s}\left(1-\frac{ml_h}{2\pi r_0}\right)+\frac{\varepsilon_{hlim}ml_h}{2\pi} \tag{32}$$

4. Case studies

In this section, two case studies illustrating the application of all equations needed to construct the SCC for the circumferential yielding lining are carried out. Generally, the computation of SCC for the circumferential yielding lining involves the following parameters: tunnel radius r_0, lining thickness t_s, shotcrete elastic modulus E_s, the number (m) and length (l_h) of highly deformable element, and its mechanical parameters (E_{h1}, σ_y, ε_{hy}, $E_{h3,i}$, $\varepsilon_{h3,i}$ and ε_{hlim}). These mechanical parameters of highly deformable element can be easily determined based on its load–strain curve.

The first case study involves a circular tunnel of radius $r_0=6$ m. The reduced elastic modulus of shotcrete E_s is equal to 23 GPa. The thickness of shotcrete lining t_s is 20 cm. The number (m) and length (l_h) of highly deformable element integrated into shotcrete lining are 9 and 40 cm, respectively. The elastic modulus (E_{h1}) and yield stress (σ_y) of highly deformable element are 510 MPa and 8.5 MPa, respectively. In addition, the maximum strain ε_{hlim} of highly deformable element is equal to 50%. The stress–strain relationship of highly deformable element is shown in Fig. 4. According to Wu et al. (2020c), the whole deforming process of highly deformable element was divided into two stages including elastic stage (I) and yielding stage (II), as shown in red dashed lines in Fig. 4, where the compaction stage (III) has not been considered. Herein, in order to perform a comparison with Wu et al. (2020c)'s result, two deforming stages of highly deformable element are assumed as well.

Based on the solution proposed in this study, SCC for the circumferential yielding lining is shown in Fig. 5. It can be seen that a good agreement is achieved between the proposed solution and Wu et al. (2020c)'s result. As shown in Fig. 5, the whole load–displacement curve of circumferential yielding lining can be divided into three parts due to the existence of highly deformable element. The highly deformable elements begin to yield when the lining pressure $p_i=0.283$ MPa corresponding to the circumferential stress of lining $\sigma_\theta=8.5$ MPa. The displacement of lining is about 124 mm without an increase of lining pressure in the yielding stage. However, after highly deformable elements become practically rigid, the lining pressure rapidly increases to 0.84 MPa (the bearing

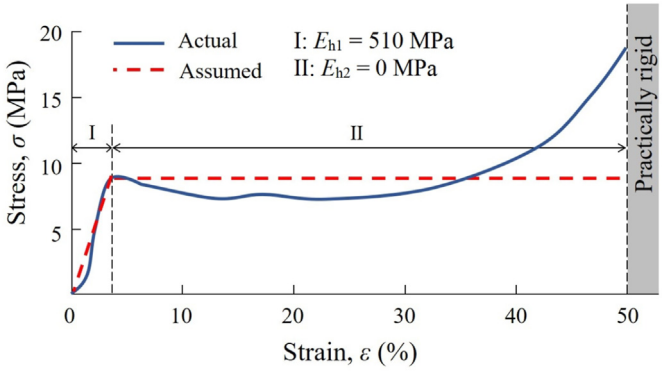

Fig. 4. Actual and assumed stress–strain curves for HidCon element (Barla et al., 2012; Wu et al., 2020c).

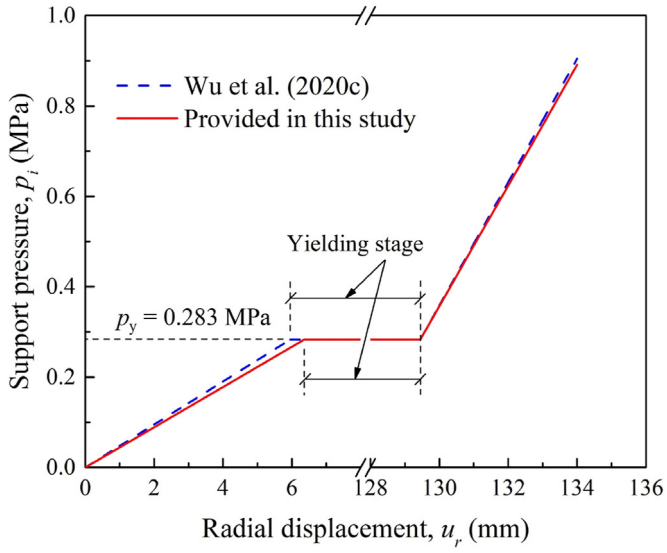

Fig. 5. Comparison of support characteristic curve between results of Wu et al. (2020c) and this study.

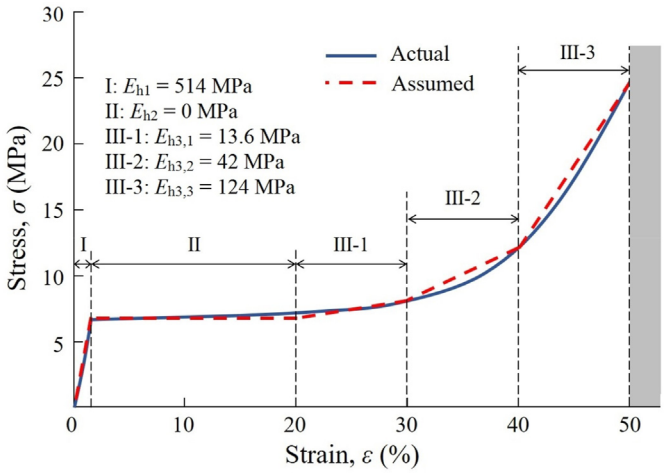

Fig. 6. Actual (Solexperts, 2007) and assumed stress–strain curves for high ductility concrete element.

capacity of C25 shotcrete lining) with the lining radial displacement increasing by approximately 4 mm.

In Wu et al. (2020c)'s solution, based on the principle of equivalent deformation, the circumferential yielding lining was processed into a "homogenized lining" and the corresponding support stiffness equations were provided. In order to obtain the SCC for the circumferential yielding lining, a further calculation based on the support stiffness equations is necessary in this study. Because in Wu et al. (2020c)'s solution, the Poisson's ratios of shotcrete and highly deformable elements were involved and they only used the Poisson's ratio of shotcrete to represent the homogenized lining for simplification. This may lead to slight differences in SCCs in Fig. 5. In addition, as previously mentioned, Wu et al. (2020c) have not taken the compaction stage of highly deformable element into consideration and they assumed that the highly deformable element only experienced elastic and yielding stages. However, it can be observed from Fig. 5 that the nonlinear compaction stage for the highly deformable element has started at the strain of approximately 30% and lasted till the strain of 50%. The maximum stress value of highly deformable element was up to about 20 MPa, which was highly larger than its yield stress of 8.5 MPa. Obviously, if the compaction stage of highly deformable element is ignored, it will result in the waste of material's actual strength.

The other case study involves a circular tunnel of radius $r_0 = 4.75$ m. The shotcrete elastic modulus E_s is reduced to 10 GPa and the thickness t_s of shotcrete lining is 25 cm. The number of highly deformable element (m) equals 4 and the length of each element is l_h = 15 cm. In this case study, the compaction stage of highly deformable element is considered and the processing scheme of its stress–strain curve is shown in Fig. 6. It can been seen from Fig. 6 that in the element compaction stage, it is sufficient to process this nonlinear stress–strain curve as three linear sub-curves in order to well describe its deforming behavior. The yield stress (σ_y) and maximum strain (ε_{hlim}) of highly deformable element are 7 MPa and 50%, respectively. Based on the element stress–strain curve, its other mechanical parameters involved in the SCC computation can be determined, that is E_{h1} = 514 MPa, ε_{hy} = 20%, $E_{h3,1}$ = 13.6 MPa, $\varepsilon_{h3,1}$ = 30%, $E_{h3,2}$ = 42 MPa, $\varepsilon_{h3,1}$ = 40% and $E_{h3,3}$ = 124 MPa.

The SCC for the circumferential yielding lining in this case is shown in Fig. 7, and that based on the proposed solution in this study is also potted in red line. Using the same parameters, Ramoni and Anagnostou (2011) carried out a numerical investigation and obtained the SCC indicated as blue dashed line in Fig. 7. It can be observed from Fig. 7 that the SCC obtained in this study well matches the numerical result obtained by Ramoni and Anagnostou (2011). The highly deformable element yields at the lining pressure p_i = 0.368 MPa. Besides, it can be found that even in the compaction stage, the elastic modulus of highly deformable element is still significantly smaller than that of shotcrete. This indicates that in the compaction stage, highly deformable elements can play a good role in releasing surrounding rock deformation as well. Based on the results in Fig. 7, the lining is able to radially displace approximately 40 mm with pressure increasing by 0.93 MPa when the highly deformable elements enter compaction stage.

Ramoni and Anagnostou (2011), based on numerical approach, investigated the mechanical response of circumferential yielding lining in a squeezing tunnel. As accepted, the tunnel performance could be well evaluated after the correct input of tunnel geometry parameters, and rock and support parameters used in numerical analysis. However, Ramoni and Anagnostou (2011) have not established a clear design method for circumferential yielding lining, which may be unable to greatly promote this novel support system in squeezing tunnels. In this study, a detailed analytical computation of SCC for circumferential yielding lining is provided, where few assumptions are made and the actual deformation behavior of highly deformable element is fully considered. The proposal of equations for determining the SCC of circumferential yielding lining can accelerate the implementation of CCM in preliminary tunnel support design. Certainly, it is also very helpful for the other sophisticated tunnel design and analysis.

In summary, the good applications of proposed equations for the SCC of circumferential yielding lining in the above two cases indicate the effectiveness and reliability of theoretical derivation in this study.

5. Parametric investigation and discussion

Based on the proposed equations for the SCC of circumferential yielding lining, it is very convenient to carry out corresponding parametric investigation. For the circumferential yielding lining, its distinguished support performance largely depends on the characteristic of highly deformable element. In this section, the

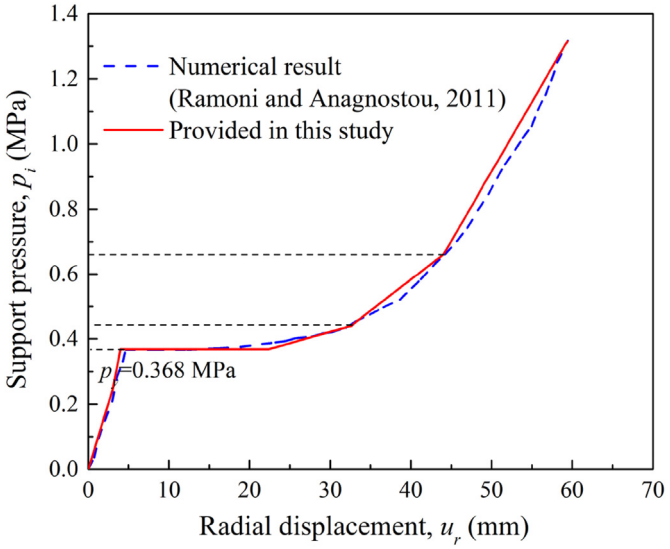

Fig. 7. Comparison of support characteristic curve between results of Ramoni and Anagnostou (2011) and this study.

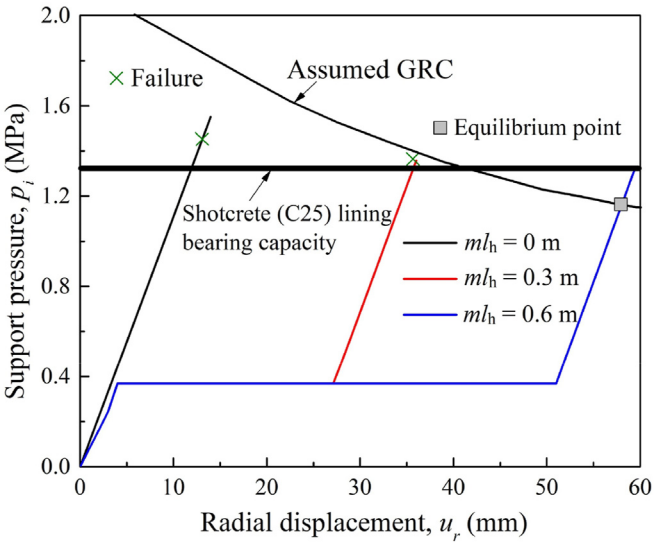

Fig. 9. Influence of highly deformable element length.

sensitivity of sub-division in the element compaction stage and the influence of element length are investigated, respectively.

5.1. Sensitivity of sub-division in the compaction stage

How does the sub-division of the element compaction stage affect the SCC and support effect? As shown in Fig. 8, the SCCs are plotted with sub-divisions $i = 0$, 1 and 3, respectively, where $i = 0$ indicates that the compaction stage of highly deformable element is not considered and the element yielding stage ends at its maximum strain achieved. In addition, other parameters involved in this analysis are all taken from the second case in Section 4.

As illustrated in Fig. 8, the sub-division of the element compaction stage has a significant influence on the SCC for circumferential yielding lining. Assuming that an equilibrium point between ground and support is achieved during the compaction period, the implementation of CCM in the above-mentioned three cases is shown in Fig. 8. Noting that in the case without considering the element compaction stage, the equilibrium point is achieved after the element yielding stage is completed. Obviously, support pressure p_i is reduced to the minimum value when the element compaction stage is not considered. In comparison, the maximum support pressure appears under the condition of $i = 1$, and the support pressure with $i = 3$ is in between those of the other two cases. Based on the results in Fig. 8, it is safe to conclude that when $i > 1$, the support pressure at the equilibrium point should range between those obtained in the cases of $i = 1$ and 0 (without considering the compaction stage). Of course, when an equilibrium point between ground and support is obtained during the element compaction period, it is very necessary to make the sub-curves describe the element deforming behavior as real as possible.

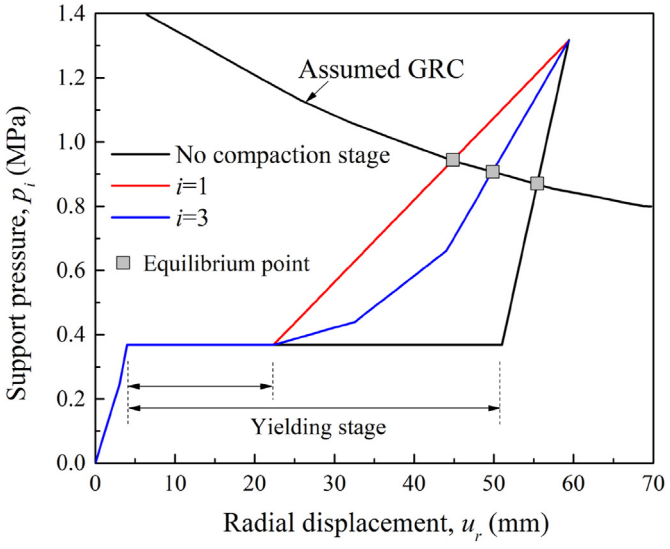

Fig. 8. Influence of sub-division of compaction stage of highly deformable element.

Interestingly, from the results in Fig. 8, if compaction deformation of highly deformable elements has been completed and an equilibrium point between ground and support has not been achieved yet, the following SCC in three cases will become the same. This indicates that it is not very important to carry out careful sub-division of element compaction stage and a same support equilibrium point will be obtained in all cases.

5.2. Influence of length of highly deformable elements

Herein, the influence of element length on the SCC is investigated. As shown in Fig. 9, these SCCs are drawn for element length $ml_h = 0$ m, 0.3 m and 0.6 m, respectively. Note that the element compaction stage is not considered and other related parameters are also taken from the second case in Section 4.

From the results in Fig. 9, the SCC is greatly affected by the highly deformable element length. It can be seen that the lining without installing highly deformable element ($ml_h = 0$ m, that is the so-called “stiff lining”) is unable to provide sufficient support resistance to restrain ground deformations without failure. As the length of highly deformable element increases, an equilibrium

point between ground and support is achieved with smaller support pressure and larger displacement. The results in Fig. 9 show that the use of highly deformable element can well improve the performance of shotcrete lining, and it is a feasible and effective solution to deal with excessive ground deformations by increasing the length of highly deformable element. Based on experience, it should be highlighted that there is a high risk of sudden change of ground from the loosening state to instability during the deforming period of highly deformable element due to relatively small support resistance. Practically, tunnel engineers are required to determine an optimal element length instead of continuously increasing its length for the purpose of smaller support pressure.

6. Conclusions

Circumferential yielding lining uses the strong deformability of highly deformable elements to release surrounding rock deformation without damaging shotcrete lining. The deforming process of highly deformable element is divided into three stages including elastic, yielding and compaction stages. Specially, in its compaction stage, the stress-strain curve is processed as several linear subcurves due to obvious nonlinear characteristic. The closure of circumferential yielding lining can be then divided into four stages. The first is induced by elastic deformations of shotcrete lining and highly deformable elements. The second is totally caused by element plastic shortening as the stress in the lining reaches the element yield stress. In the third stage, lining closure is triggered by element compaction shortening and elastic deformation of shotcrete lining. Finally, after experiencing the limit strain, the shotcrete lining continues to work until failure.

The analytical computation of SCC for circumferential yielding lining is presented, and the accurate equations for constructing SCC in different stages are provided. The use of SCC for circumferential yielding lining involves the parameters of tunnel radius, lining thickness, shotcrete elastic modulus, and the number, length and mechanical parameters of highly deformable element. The solution derived can be easily reduced to the previous simple case that does not consider the element compaction stage, which possibly causes the waste of material's actual strength.

Based on the construction of SCC for circumferential yielding lining, engineers can find that it is important to consider the sensitivity of sub-division of element in compaction stage if an equilibrium point between ground and support is achieved during compaction period. As the length of highly deformable element increases, that equilibrium point can be achieved with lower support pressure.

Declaration of competing interest

The authors declare that they have no known competing financial interests or personal relationships that could have appeared to influence the work reported in this paper.

Acknowledgments

This work is supported by National Natural Science Foundation of China (Grant Nos. 11872287 and 51908431), and Fund of Shaanxi Key Research and Development Program (Grant No. 2019ZDLGY01-10).

References

Asef, M.R., Reddish, D.J., Lloyd, P.W., 2000. Rock–support interaction analysis based on numerical modelling. Geotech. Geol. Eng. 18 (1), 23–37.
Aygar, E.B., 2020. Evaluation of new Austrian tunnelling method applied to Bolu tunnel's weak rocks. J. Rock Mech. Geotech. Eng. 12 (3), 541–556.
Barla, G., Bonini, M., Semeraro, M., 2011. Analysis of the behaviour of a yield-control support system in squeezing rock. Tunn. Undergr. Space Technol. 26 (1), 146–154.
Barla, G., Debernardi, D., Sterpi, D., 2012. Time-dependent modeling of tunnels in squeezing conditions. Int. J. GeoMech. 12 (6), 697–710.
Barla, G., 2016. Full-face excavation of large tunnels in difficult conditions. J. Rock Mech. Geotech. Eng. 8 (3), 294–303.
Bonini, M., Barla, G., 2012. The Saint Martin La Porte access adit (Lyon–Turin Base tunnel) revisited. Tunn. Undergr. Space Technol. 30, 38–54.
Brown, E.T., Bray, J.W., Ladanyi, B., Hoek, E., 1983. Ground response curves for rock tunnels. J. Geotech. Eng. 109 (1), 15–39.
Cantieni, L., Anagnostou, G., 2009. The interaction between yielding supports and squeezing ground. Tunn. Undergr. Space Technol. 24 (3), 309–322.
Carranza-Torres, C., 2003. Dimensionless graphical representation of the exact elasto-plastic solution of a circular tunnel in a Mohr-Coulomb material subject to uniform far-field stresses. Rock Mech. Rock Eng. 36 (3), 237–253.
Carranza-Torres, C., Engen, M., 2017. The support characteristic curve for blocked steel sets in the convergence-confinement method of tunnel support design. Tunn. Undergr. Space Technol. 69, 233–244.
Chu, Z., Wu, Z., Liu, B., Liu, Q., 2019. Coupled analytical solutions for deep-buried circular lined tunnels considering tunnel face advancement and soft rock rheology effects. Tunn. Undergr. Space Technol. 94, 103111.
Chu, Z., Wu, Z., Liu, Q., Liu, B., Sun, J., 2021. Analytical solution for lined circular tunnels in deep viscoelastic burgers rock considering the longitudinal discontinuous excavation and sequential installation of liners. J. Eng. Mech. 147 (4), 04021009.
De La Fuente, M., Taherzadeh, R., Sulem, J., Nguyen, X.S., Subrin, D., 2019. Applicability of the convergence-confinement method to full-face excavation of circular tunnels with stiff support system. Rock Mech. Rock Eng. 52 (7), 2361–2376.
Deng, Y., Xie, J., Li, S., 2020. Research and application of support resistant limiting dampers in the deep-buried large-section loess tunnel. Adv. Civ. Eng. 2020, 8841703.
Fan, S., Song, Z., Zhang, Y., Liu, N., 2020. Case study of the effect of rainfall infiltration on a tunnel underlying the roadbed slope with weak inter-layer. KSCE J. Civ. Eng. 24 (5), 1607–1619.
Hammer, A.L., Hasanpour, R., Hoffmann, C., Thewes, M., 2018. Numerical analysis of interaction behavior of yielding supports in squeezing ground. In: Cardoso, A.S., Borges, J.L., Costa, P.A., Gomes, A.T., Marques, J.C., Vieira, C.S. (Eds.), Numerical Methods in Geotechnical Engineering IX: Proceedings of the 9th European Conference on Numerical Methods in Geotechnical Engineering (NUMGE 2018). CRC Press, London, UK.
Hasanpour, R., Hammer, A.L., Thewes, M., 2018. Analysis of multilateral interaction between shotcrete, yielding support and squeezing ground by means of two different numerical methods. In: ITA-AITES World Tunnel Congress 2018. Dubai World Trade Centre, Dubai, United Arab Emirates.
He, S., Lai, J., Zhong, Y., Wang, K., Xu, W., Wang, L., Liu, T., Zhang, C., 2021. Damage behaviors, prediction methods and prevention methods of rockburst in 13 deep traffic tunnels in China. Eng. Fail. Anal. 121, 105178.
Kabwe, E., Karakus, M., Chanda, E.K., 2020a. Proposed solution for the ground reaction of non-circular tunnels in an elastic-perfectly plastic rock mass. Comput. Geotech. 119, 103354.
Kabwe, E., Karakus, M., Chanda, E.K., 2020b. Time-dependent solution for non-circular tunnels considering the elasto-viscoplastic rockmass. Int. J. Rock Mech. Min. Sci. 133, 104395.
Kovári, K., 2009. Design methods with yielding support in squeezing and swelling rocks. In: ITA-AITES World Tunnel Congress 2009. Budapest, Hungary.
Kumasaka, H., 2007. Numerical computation of support characteristic curves for use in tunnel support design and their application to the characteristic curve method. Int. J. JCRM 3 (1), 1–6.
Langford, J.C., Vlachopoulos, N., Diederichs, M.S., 2016. Revisiting support optimization at the Driskos tunnel using a quantitative risk approach. J. Rock Mech. Geotech. Eng. 8 (2), 147–163.
Lu, W., Sun, H., 2020. Study on support characteristic curve of concrete-filled steel tubular arch in underground support. Structure 27, 1809–1819.
Lu, W., Zhao, D., Li, D.B., Jiang, H.T., 2021. Evaluation on anchoring force demands of typical damaged rammed earth city wall sites under earthquake. Arab. J. Geosci. 14, 692.
Moritz, B., 2011. Yielding elements – requirements, overview and comparison. Geomech. Tunn. 4 (3), 221–236.
Oke, J., Vlachopoulos, N., Diederichs, M., 2018. Improvement to the convergence-confinement method: inclusion of support installation proximity and stiffness. Rock Mech. Rock Eng. 51 (5), 1495–1519.
Oreste, P.P., 2003a. Analysis of structural interaction in tunnels using the convergence-confinement approach. Tunn. Undergr. Space Technol. 18 (4), 347–363.

Oreste, P.P., 2003b. A procedure for determining the reaction curve of shotcrete lining considering transient conditions. Rock Mech. Rock Eng. 36 (3), 209–236.
Panet, M., 1995. Le calcul des tunnels par la méthode convergence-confinement. Presses de l'Ecole Nationale des ponts et chaussées, Paris, France (in French).
Paraskevopoulou, C., Diederichs, M., 2018. Analysis of time-dependent deformation in tunnels using the convergence-confinement method. Tunn. Undergr. Space Technol. 71, 62–80.
Qiu, W., Wang, G., Gong, L., Shen, Z., Li, C., Dang, J., 2018. Research and application of resistance-limiting and energy-dissipating support in large deformation tunnel. Chin. J. Rock Mech. Eng. 37 (8), 1785–1795 (in Chinese).
Radončić, N., Schubert, W., Moritz, B., 2009. Ductile support design. Geomech. Tunn. 2 (5), 561–577.
Ramoni, M., Anagnostou, G., 2011. The interaction between shield, ground and tunnel support in TBM tunnelling through squeezing ground. Rock Mech. Rock Eng. 44, 37–61.
Rodríguez, R., Díaz-Aguado, M.B., 2013. Deduction and use of an analytical expression for the characteristic curve of a support based on yielding steel ribs. Tunn. Undergr. Space Technol. 33, 159–170.
Sakai, K., Schubert, W., 2019. Study on ductile support system by means of convergence confinement method. In: 5th ISRM Young Scholars' Symposium on Rock Mechanics and International Symposium on Rock Engineering for Innovative Future. Okinawa, Japan.
Schubert, W., Brunnegger, S., Staudacher, R., Wenger, J., 2018. Further development of yielding elements and connecting elements for shotcrete. Geomech. Tunn. 11 (5), 575–581.
Solexperts, A.G., 2007. HIDCON-elemente im Tunnelbau (Mönchaltorf).
Sun, Y., Li, G., Zhang, N., Chang, Q., Xu, J., Zhang, J., 2021. Development of ensemble learning models to evaluate the strength of coal-grout materials. Int. J. Min. Sci. Tech. 31 (2), 153–162.
Tian, H., Chen, W., Yang, D., Wu, G., Tan, X., 2016. Numerical analysis on the interaction of shotcrete liner with rock for yielding supports. Tunn. Undergr. Space Technol. 54, 20–28.
Tian, H.M., Chen, W.Z., Tan, X.J., Yang, D.S., Wu, G.J., Yu, J.X., 2018. Numerical investigation of the influence of the yield stress of the yielding element on the behaviour of the shotcrete liner for yielding support. Tunn. Undergr. Space Technol. 73, 179–186.
Thut, A., Naterop, D., Steiner, P., Stolz, M., 2006. Tunnelling in squeezing rock-yielding elements and face control. In: 8th International Symposium on Tunnel Construction and Underground Structures. Lubljana, Slovenia.
Verient, M., Kluckner, A., Radoncic, N., Schubert, W., 2015. Investigations on telescope yielding elements with porous filling. In: ISRM Regional Symposium – EUROCK2015. Salzburg, Austria, pp. 1169–1174.
Wang, Y., 1996. Ground response of circular tunnel in poorly consolidated rock. J. Geotech. Eng. 122 (9), 703–708.
Wang, Z.C., Shi, Y.F., Xie, Y.L., Zhang, M.Z., Liu, T., Li, C., 2021. Support characteristic of a novel type of support in loess tunnels using the convergence-confinement method. Int. J. GeoMech. 21 (10), 06021026.
Wu, K., Shao, Z., 2019. Study on the effect of flexible layer on support structures of tunnel excavated in viscoelastic rocks. J. Eng. Mech. 145 (10), 04019077.
Wu, K., Shao, Z., Qin, S., Zhao, N., 2019. Mechanical analysis of tunnels supported by yieldable steel ribs in rheological rocks. Geomech. Eng. 19 (1), 61–70.
Wu, K., Shao, Z., Qin, S., Zhao, N., Hu, H., 2020a. Analytical-based assessment of effect of highly deformable elements on tunnel lining within viscoelastic rocks. Int. J. Appl. Mech. 12 (3), 2050030.
Wu, K., Shao, Z., Qin, S., 2020b. A solution for squeezing deformation control in tunnels using foamed concrete: a review. Construct. Build. Mater. 257, 119539.
Wu, K., Shao, Z., Qin, S., 2020c. An analytical design method for ductile support structures in squeezing tunnels. Archiv. Civ. Mech. Eng. 20 (3), 91.
Xu, C., Xia, C., 2021. A new large strain approach for predicting tunnel deformation in strain-softening rock mass based on the generalized Zhang-Zhu strength criterion. Int. J. Rock Mech. Min. Sci. 143, 104786.
Yan, Q., Li, S.C., Xie, C., Li, Y., 2018. Analytical solution for bolted tunnels in expansive loess using the convergence-confinement method. Int. J. GeoMech. 18 (1), 04017124.

Kui Wu obtained his PhD degree at Xi'an University of Architecture and Technology, China. He is presently working as a postdoctoral research fellow at the same university. He was a visiting scholar at Curtin University, Australia. His main research interests include soft rock rheological property, advanced underground excavation techniques and novel support structures. He has published more than 10 SCI papers in high-impact international journals.